

## Letter

# Measurement of delayed neutron yields and time spectra from 1 GeV protons interacting with thick $^{\text{nat}}\text{Pb}$ targets

D. Ridikas<sup>1,a</sup>, A. Barzakh<sup>2</sup>, V. Blideanu<sup>1</sup>, J.C. David<sup>1</sup>, D. Doré<sup>1</sup>, D. Fedorov<sup>2</sup>, X. Ledoux<sup>3</sup>, F. Moroz<sup>2</sup>, V. Panteleev<sup>2</sup>, R. Plukienė<sup>4</sup>, A. Plukis<sup>4</sup>, A. Prévost<sup>1</sup>, O. Shcherbakov<sup>2</sup>, and A. Vorobyev<sup>2</sup>

<sup>1</sup> CEA Saclay, DSM/DAPNIA, 91191 Gif-Sur-Yvette, France

<sup>2</sup> Petersburg Nuclear Physics Institute (PNPI), 188350 Gatchina, Leningrad district, Russia

<sup>3</sup> CEA/DAM Ile-de-France, DPTA/SPN, 91680 Bruyères-le-Châtel, France

<sup>4</sup> Institute of Physics, Savanoriu pr. 231, 02300, Vilnius, Lithuania

Received: 5 March 2007 / Revised: 6 April 2007

Published online: 3 May 2007 – © Società Italiana di Fisica / Springer-Verlag 2007

Communicated by J.A. Aystö

**Abstract.** In this paper we present for the first time the measured delayed neutron (DN) yields and time spectra from high-energy protons interacting with thick  $^{\text{nat}}\text{Pb}$  targets. The 1 GeV protons from the accelerator impinged on targets of different thicknesses producing a huge number of spallation-fission products, some of which can be DN precursors. After the beam is switched off, the DNs were detected with optimized  $^3\text{He}$  counter. The production yields of light DN precursors as  $^{17}\text{N}$  and “usual” fission products as  $^{87}\text{Br}$  and  $^{88}\text{Br}$ , which dominate the total DN activity, are obtained both for thin and thick targets. These new data are of great interest for the new generation high-power spallation targets based on liquid-metal technologies. Our findings also should help to constrain the physics models within the simulations codes.

**PACS.** 25.40.Sc Spallation reactions – 25.85.Ge Charged-particle-induced fission

## Introduction

The next-generation spallation neutron sources, neutrino factories or radioactive ion beam production facilities currently being designed and constructed around the world will require an increase of the average proton beam power on target by a few orders of magnitude. Increased proton beam power up to a few MW requires the use of liquid-metal targets such as Hg, Pb, or Pb-Bi. Radioactive nuclides produced in such targets are transported into hot cells, into pumps with radiation-sensitive components and electronics, etc. Due to a short transit time, typically 10–20 s, a significant amount of the DN precursor activity can be accumulated in the target fluid contributing significantly to the activation and dose rates. This phenomenon was discussed in detail in ref. [1] including the estimation of the expected DN flux and corresponding time spectra in the case of the MegaPie liquid-metal spallation target at PSI (Switzerland) [2]. In ref. [1] it was also demonstrated that the final estimates of DNs were extremely model-dependent within the multi-particle transport code MCNPX [3].

The goal of this work was to measure the DN production from high-energy fission-spallation reactions on  $^{\text{nat}}\text{Fe}$ ,  $^{\text{nat}}\text{Pb}$  and  $^{209}\text{Bi}$  targets of variable thicknesses. Here we present the 1st experimental results on the absolute DN yields and time spectra from 1 GeV protons interacting with thick  $^{\text{nat}}\text{Pb}$  targets. Corresponding predictions with commonly employed MCNPX [3] and PHITS [4] reaction-transport codes are also performed leading to some recommendations related to the use of these tools. More detailed analysis including data obtained from the  $^{209}\text{Bi}$  and  $^{\text{nat}}\text{Fe}$  targets will be reported elsewhere.

## Experimental

A schematic view of the experiment, realized at PNPI Gatchina (Russia), is shown in fig. 1. 1 GeV protons delivered by the PNPI synchrocyclotron impinged on the  $^{\text{nat}}\text{Pb}$  targets of 10 cm diameter and 6 different thicknesses, namely 0.5, 5, 10, 20, 40 and 55 cm. The repetition rate of the accelerator was 50 Hz and the average proton current on the target was around 20 nA. Long (300 s), intermediate (20 s) and short (350  $\mu\text{s}$  — a single macro-pulse)

<sup>a</sup> e-mail: ridikas@cea.fr

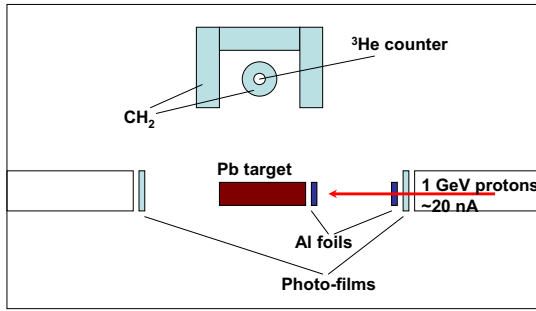


**Fig. 1.** A schematic view of the experimental setup to measure DNs with the proton beam line (coming from the right), the Pb target (placed at the centre) and  $^3\text{He}$  counter (seen above the target).

irradiation periods were used to optimize the extraction of different time parameters of DN groups.

The emitted DNs were detected with the standard  $^3\text{He}$  detector following specific irradiation periods after the beam was switched off. The  $^3\text{He}$  counter was surrounded by a 5 cm thick polyethylene ( $\text{CH}_2$ ) to increase the neutron detection efficiency in terms of neutron moderation and coated by 1 mm  $^{\text{nat}}\text{Cd}$  foils (see fig. 1) to avoid the background due to the thermal neutrons. The detector optimization was performed using full-scale Monte Carlo simulations with MCNPX [3]. The detector was calibrated with a standard  $^{252}\text{Cf}$  neutron source, and its efficiency was reproduced within 6% by MCNPX. The Monte Carlo simulations have also shown that the relative efficiency variation of the DN detector to the expected neutron energies, typically from 0.1 MeV to 1.2 MeV, was less than 9%.

The proton beam was focused to a spot of about 2 cm in diameter and was periodically verified using photo-films (see fig. 1). For each target the beam intensity was permanently monitored with relative errors from 8 to 11% by activation of  $^{27}\text{Al}$  foils and the  $\gamma$ -spectroscopy off-line from the  $^7\text{Be}$ ,  $^{22}\text{Na}$  and  $^{24}\text{Na}$  activity. The HPGe detector was used for this purpose, its calibration being done with standard  $^{60}\text{Co}$ ,  $^{137}\text{Cs}$ ,  $^{139}\text{Ba}$  and  $^{152}\text{Eu}$  gamma sources.

Each individual irradiation-decay cycle was recorded on-line and after verification was summed off-line to accumulate the statistics. Note that the  $^3\text{He}$  detector was saturated during the irradiation and came back to “normal” operation only in 35–40 ms period after the beam switch-off. The verification of the individual cycles was necessary to cross check if this relaxation time of the neutron counter was of the same order of magnitude during the entire experiment. Using the same technique, some measurements without target and with iron or concrete brick samples were also performed to characterize the active background contribution due to the environment of the experimental area. During these test measurements we observed only two dominating decay periods of  $T_{1/2} \sim 4.2\text{ s}$  and  $\sim 0.18\text{ s}$ , which we tentatively attributed to the reaction products  $^{17}\text{N}$  and  $^9\text{Li}$  with  $T_{1/2} = 4.173\text{ s}$  and  $T_{1/2} = 0.178\text{ s}$ , respectively. Indeed, these two DN precursors can be produced in the reactions induced by 1 GeV protons on different targets as Al, Cu, Ni, W or other materials [5]. It is impor-

tant to note that no longer half-lives were observed during these test irradiations. Once the irradiations with  $^{\text{nat}}\text{Pb}$  targets started, we noticed that the DN decay curves also extended to the half-lives longer than  $\sim 4.2\text{ s}$ , which are characteristic for the neutron-rich fission products only [6]. This observation was already mentioned in ref. [5] giving only the higher upper limit of  $\sim 24\ \mu\text{b}$  for the production of long-lived DN emitters.

Analysis of the DN decay curves for all  $^{\text{nat}}\text{Pb}$  thicknesses and with identical long irradiation-decay periods of 300 s–300 s was performed by fitting the data with the sum of decay exponentials using the standard TMinuit class implemented in the ROOT toolkit [7]. The following expression, representing the decay after long irradiation [6], was employed to obtain the  $\{a_i; \lambda_i\}$  values:

$$\text{DN}(t) = \sum_i a_i \exp(-\lambda_i t) (1 - \exp(-\lambda_i T_{\text{irr}})) + C, \quad (1)$$

with  $\lambda_i = \ln 2 / T_{1/2}^i$ ,  $C$  — a constant background contribution, and the irradiation time  $T_{\text{irr}} = 300\text{ s}$ . Historically, the origin of 6–8 groups of DNs is somewhat artificial the goal being to reproduce the DN decay spectra with the minimum number of exponentials. Contrary to the conventional 6- or 8-group approaches to reproduce the DN decay curves from neutron-induced fission on actinides [6], only 4 terms of the above expression were sufficient in our case. Note that the half-lives for these 4 terms correspond exactly to the previously identified reaction products, namely  $^9\text{Li}$  and  $^{17}\text{N}$  and two fission fragments  $^{87}\text{Br}$  and  $^{88}\text{Br}$  (with  $T_{1/2} = 55.6\text{ s}$  and  $T_{1/2} = 16.29\text{ s}$ , respectively). In order to confirm these findings we analyzed in detail the earlier experimental work on isotopic yields of reaction products from 1 GeV proton-induced reactions on Pb or neighboring targets [5,8]. Indeed, this preparatory work permitted to restrain a number of half-lives. In the case of the 2nd group [6], the DN precursors as  $^{136}\text{Te}$  ( $T_{1/2} = 17.5\text{ s}$ ),  $^{137}\text{I}$  ( $T_{1/2} = 24.5\text{ s}$ ), and  $^{141}\text{Cs}$  ( $T_{1/2} = 24.9\text{ s}$ ) with comparable half-lives can be neglected due to their very small production cross-sections (2 orders of magnitude lower than expected for  $^{88}\text{Br}$ ) [8]. Equally, the contribution of  $^{92}\text{Rb}$  ( $T_{1/2} = 4.49\text{ s}$ ),  $^{93}\text{Rb}$  ( $T_{1/2} = 5.84\text{ s}$ ) and  $^{94}\text{Rb}$  ( $T_{1/2} = 2.70\text{ s}$ ) to the 3rd group [6] is negligible.

The data accumulated for the 55 cm thick  $^{\text{nat}}\text{Pb}$  target are presented together with the fits of the exponential sum in fig. 2. Similar quality fits using the same 4 terms in the exponential sum, *i.e.* with four half-lives fixed to those of  $^9\text{Li}$ ,  $^{17}\text{N}$ ,  $^{87}\text{Br}$  and  $^{88}\text{Br}$ , were successfully obtained for all target thicknesses [9] (not presented in this work).

## Discussion

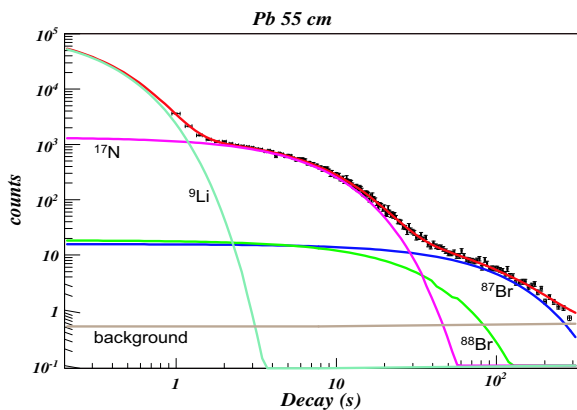
A few interesting findings should be highlighted. First of all, the DN contribution from light-mass products as  $^9\text{Li}$  and  $^{17}\text{N}$  dominates over the DN contribution from fission products (fig. 2). This is understandable if the  $p(1\text{ GeV})+\text{Pb}$  fission cross-section of only  $157 \pm 26\text{ mb}$  [8] is

**Table 1.** The DN precursor yields  $Y^i$  (atoms per proton) as a function of the target thickness from  $p(1\text{ GeV}) + {}^{\text{nat}}\text{Pb}$ . The relative ratios of data over PHITS code predictions are also provided.

Target thickness, cm	${}^{17}\text{N}$ , atoms/p ( $\times 10^{-6}$ )		${}^{87}\text{Br}$ , atoms/p ( $\times 10^{-6}$ )		${}^{88}\text{Br}$ , atoms/p ( $\times 10^{-6}$ )	
	Data	Data/PHITS	Data	Data/PHITS	Data	Data/PHITS
5	$81.4 \pm 8.8$	2.4	$6.5 \pm 1.9$	1.7	$4.9 \pm 2.2$	0.8
10	$116.9 \pm 9.1$	2.3	$16.9 \pm 2.1$	1.3	$9.0 \pm 2.1$	0.9
20	$126.0 \pm 15.6$	1.5	$34.1 \pm 4.5$	1.1	$22.0 \pm 4.1$	0.6
40	$125.2 \pm 14.9$	1.3	$45.0 \pm 5.8$	1.2	$20.8 \pm 3.9$	0.9
55	$125.2 \pm 15.1$	1.3	$52.9 \pm 6.5$	1.1	$22.9 \pm 3.8$	0.9

**Table 2.** Production cross-sections of some of the DN precursors from  $p(1\text{ GeV}) + {}^{\text{nat}}\text{Pb}$ . Error bars in the case of model predictions are statistical.

$\sigma$ , $\mu\text{b}$	This work	Old data	PHITS (NMTC/JAM + GEM)	MCNPX2.5.0 (INCL4 + ABLA)
${}^{17}\text{N}$	$493 \pm 86$	–	$249 \pm 17$	–
${}^{87}\text{Br}$	$40 \pm 12$	$33 \pm 20$ [8]	$52 \pm 8$	$65 \pm 8$
${}^{88}\text{Br}$	$30 \pm 11$	–	$8 \pm 3$	$18 \pm 4$

**Fig. 2.** (Colour on-line) Accumulated DN decay curve from  $p(1\text{ GeV}) + \text{Pb}$ : the experimental data (points), contributions due to the total (red solid line) and individual DN precursors (see labels) are shown separately.

compared to the  ${}^9\text{Li}$  and  ${}^{17}\text{N}$  production cross-sections expected between 500 mb and 1000 mb (see fig. 3 in ref. [5]). Therefore, this “unusual” DN emission dominates the DN decay curve for Pb and Bi targets up to the cooling time of 10–20 s (see fig. 2). For longer decay times, say 50–100 s, the long-lived DN precursors, being “usual” fission products as  ${}^{88}\text{Br}$  and  ${}^{87}\text{Br}$ , remain the only contributors to the DN activity. Note that this information is very important in the case of high-power liquid-metal targets, where the liquid metal makes the “round trip” typically in the period of 10–30 s (*e.g.*,  $\sim 20$  s in the case of MegaPie [1, 2]).

Thanks to the efficiency determination of the  ${}^3\text{He}$  counter and to the proton beam intensity monitoring, it was possible to extract the DN yields in absolute values. In brief, once the  $\text{DN}(t)$  is parameterised during the fitting procedure (see fig. 2 and eq. (1)) and when  $t$  approaches

zero, one obtains  $\text{DN}(t \rightarrow 0) = \sum_i a_i + C$ . Here, the following expression can be employed to calculate the individual DN yields:  $P_n^i Y^i = a_i / (\varepsilon_{\text{He-3}} I_p \Delta t_{\text{ch}} N_{\text{cycles}})$ , with  $P_n^i$  being the DN emission probability,  $Y^i$  —the individual DN precursor yield (atoms per incident proton),  $\varepsilon_{\text{He-3}}$  —the total efficiency of the  ${}^3\text{He}$  counter (events per emitted source neutron),  $I_p$  —the proton beam intensity (protons per second),  $\Delta t_{\text{ch}}$  —the channel width (seconds),  $N_{\text{cycles}}$  —a number of accumulated irradiation-decay cycles.

Table 1 presents the obtained DN precursor production yields  $Y^i$  for  $i = {}^{17}\text{N}$ ,  ${}^{87}\text{Br}$  and  ${}^{88}\text{Br}$  as a function of the target thickness. Note that in addition to the uncertainties in the detector efficiency, proton beam intensity monitoring and statistical errors, we took into account systematic errors due to the fitting procedure and background contribution. We add that the extraction of  ${}^9\text{Li}$  yields was impossible due to its short half-life, which is comparable with the experimental channel width  $\Delta t_{\text{ch}} = 200$  ms.

From this data (table 1) one observes that the DN precursor yields are increasing with target thickness but some saturation is observed for targets thicker than 20–30 cm. Indeed, most of the high-energy reactions, including fission, take place in the 1st half of the stopping target. One also can notice that relative yield ratios of  ${}^{88}\text{Br}/{}^{87}\text{Br}$  and  ${}^{17}\text{N}/{}^{87}\text{Br}$  behave differently as a function of the target thickness: the 1st one is nearly constant for all thicknesses, while the 2nd one is decreasing with increasing target thickness until the saturation is reached. This can be explained in terms of two different reaction mechanisms responsible for the production of these DN precursors, namely fission (Br) and fragmentation-evaporation (N and Li), respectively. These findings are reproduced by the model predictions obtained using the PHITS code (the NMTC/JAM intra-nuclear cascade coupled to the GEM fission/evaporation model) [4] and prove that this code can predict rather accurately the formation of DN precursors.

sors in high-energy spallation-fission reactions —within a factor of 2 or better.

Using the data taken with thin targets (0.5 cm and 5.0 cm) the production cross-sections of  $^{87}\text{Br}$ ,  $^{88}\text{Br}$  and  $^{17}\text{N}$  have been extracted and are presented in table 2. Note that the increase in target thickness from 0.5 cm to 5.0 cm has shown that secondary reactions contribute less than 10% to the total production. In the same table 2 comparisons are made with PHITS [4] and MCNPX (the INCL4 intra-nuclear cascade coupled to the ABLA fission/evaporation model) [3] code predictions including some older data [8]. Note that in ref. [8]  $^{208}\text{Pb}$  and not  $^{\text{nat}}\text{Pb}$  was used, so the comparison should be done with a certain precaution. As it was mentioned earlier in the case of thick targets, PHITS gives reasonable results both for  $^{17}\text{N}$  and  $^{87,88}\text{Br}$ . MCNPX can be trusted only for  $^{87,88}\text{Br}$  since in the present version it does not allow the production of light spallation fragments as  $^{17}\text{N}$  or  $^9\text{Li}$  at all. It is worth mentioning that the  $^{17}\text{N}$  and  $^{88}\text{Br}$  cross-sections for 1 GeV protons are measured for the first time, while the uncertainty for  $^{87}\text{Br}$  is improved by a factor of 2. We add that the obtained cross-sections, measured for  $^{17}\text{N}$ ,  $^{88}\text{Br}$  and re-measured for  $^{87}\text{Br}$ , are consistent with values expected/reported in refs. [5] and [8].

## Conclusions

In this work we present for the 1st time the experimental data on measured DN yields and time spectra from 1 GeV protons interacting with thick  $^{\text{nat}}\text{Pb}$  targets. The emission of DNs is dominated by light reaction products as  $^9\text{Li}$  and  $^{17}\text{N}$  during the decay time from 0 to  $\sim 20\text{--}30$  s, while after the longer decay time the fission fragments as  $^{88}\text{Br}$  and  $^{87}\text{Br}$  are the major contributors. The DN yield production per incident proton is increasing with the target thickness and the majority of the DNs from 1 GeV protons are produced in the 1st half of the stopping target. In addition to

the DN yields, the microscopic production cross-sections of the DN precursors have been extracted for  $^{17}\text{N}$ ,  $^{87}\text{Br}$  and  $^{88}\text{Br}$ .

The above experimental observations are reproduced with the PHITS transport code, which is able to predict the production of the DN precursors within a factor of 2 or better. These new data are of great importance for the new-generation high-power spallation targets based on liquid-metal technology as well as for further development of high-energy spallation-fission-fragmentation models.

## References

1. D. Ridikas *et al.*, *Delayed Neutrons from High Energy Fission-Spallation Reactions*, in *Proceedings of the 3rd International Workshop Fission2005, 11-14 May 2005, CEA Cadarache, France*, AIP Conf. Proc. **798**, 277 (2005).
2. G.S. Bauer, M. Salvatore, G. Heusener, *MEGAPIE, a 1 MW Pilot Experiment for a Liquid Metal Spallation Target*, in *Proceedings of the 15th International Conference ICANS-XV (2000)*, edited by J. Suzuki, S. Itoh (JAERI, Tsukuba, Japan, 2001).
3. D.B. Pelowitz, *MCNPX<sup>TM</sup> USER'S MANUAL - Version 2.5.0*, LA-CP-05-0369, LANL, USA, April 2005.
4. H. Iwase *et al.*, Nucl. Instrum. Methods B **183**, 374 (2001).
5. I. Dostrovsky *et al.*, Phys. Rev. **139**, 1513 (1965).
6. W.B. Wilson, T.R. England, Prog. Nucl. Energy **41**, 71 (2002).
7. R. Brun, F. Rademaker, Nucl. Instrum. Methods A **389**, 81 (1997).
8. T. Engvist *et al.*, Nucl. Phys. A **686**, 481 (2001).
9. D. Ridikas *et al.*, *Relative Delayed Neutron Yields and Time Spectra from 1 GeV protons interacting with thick  $^{\text{nat}}\text{Pb}$  targets*, in *Proceedings of the International Conference PHYSOR2006, Vancouver, Canada, 10-14 September 2006*, ISBN: 0-89448-697-7, B104, 9 pp., CD-ROM (2006) American Nuclear Society.